◇ Monograph Excerpt ◇

# Matter Antimatter Fluctuations

## search, discovery and analysis of Bs flavor oscillations

Nuno Leonardo

*Complete work published as:*
Analysis of $B_s$ oscillations at CDF, MIT Thesis (2006)
Matter antimatter fluctuations, Monograph, LAP Lambert (2011)

# Chapter 1

# Introduction

The phenomenon of $B$–$\bar{B}$ flavor oscillations, or mixing, refers to particle-antiparticle transitions in the neutral $B$ meson systems, where $B$ can be either $B^0$ or $B_s$, formed respectively of a bottom antiquark and either a down or a strange quark. The rate at which these transformations occur is characterized by the mass difference between the two quantum states of the meson, denoted $\Delta m$. Neutral $B$ meson mixing is currently the subject of very intense research in high energy physics. As it will be seen shortly, mixing measurements address many outstanding questions relating to the standard model (SM) of particle physics. In particular it directly relates to fundamental parameters of the theory, shedding light on the processes of charge-parity (CP) violation, mass scales, and generation structure.

Experiments in the past few decades have verified the SM gauge structure of elementary particle interactions, in a comprehensive and very precise way. The flavor sector had not been explored to the same extent, and it constitutes one of the highest priorities of contemporary high energy physics. The SM serves as the current foundation for discussing flavor physics. The quark masses, their mixing and CP violation have there a common origin. Namely, they arise from Yukawa interactions with the (yet to be observed) Higgs field. However, all mass scales and their hierarchies are left unexplained, *i.e.* they are not predicted and need to be fixed by empirical inputs. This constitutes a shortcoming of the model.

There are several additional powerful experimental and phenomenological reasons to expect new physics (NP). The SM is thus often taken, a perspective we share, as a (remarkable) *effective* theory describing nature at the energy scales probed so far. Many extensions of the SM have been sought, ranging from compositeness, low or high scale supersymmetry (SUSY), grand unification (GUT), to extra dimensions and deconstruction, and string/M theories. Each of them overcomes some unsatisfactory aspects of the SM while adding considerably more unknowns.

There are theoretical hints that NP should be found at accessible energy scales. The

available experimental data exclude, however, the possibility of sizable contributions to tree-level (*i.e.* lowest order perturbation theory) SM processes. Large new contributions are most likely to be present in loop-mediated processes. This renders meson mixing a fertile ground to reveal the influence of new interactions.

The measurement of $B_s$ oscillations is thus quite interesting from a phenomenological perspective. If on the one hand the oscillation frequency is found within the expected SM region, it becomes a precision measurement providing strong constraints on the model parameters. In that case it will add to the remarkable success of the SM and further corroborate it as an effective theory at the energy scales so far probed. At the same time, it places further bounds on extensions of the SM, emphasizing that if there is NP at the TeV scale it must have a special flavor structure to satisfy the observed constraints. On the other hand, if the measurement is found incompatible with the existing SM constraints, it will constitute a direct indication of new physics. In either case, it is bound to be a most exciting result. From the experimental point of view, it is an extremely challenging endeavor and, most definitely, no less exciting.

## 1.1 Synopsis and roadmap

The large expected value of the particle–antiparticle mixing frequency makes it challenging to observe and measure the time-dependence of $B_s$ flavor oscillations. The amplitude of the oscillations is attenuated by effects resulting from background contamination of the samples, experimental resolutions on the decay proper time reconstruction, and performance limitations of the flavor tagging methods.

In the absence of such attenuation effects and further experimental complications, the probability density for an originally produced $B_s$ meson to decay at a later time $t$ as $\bar{B}_s$, or conversely, follows from basic quantum mechanics, as derived in Chapter 2, and is given simply by

$$\mathcal{P}_{B_s \to \bar{B}_s} \sim \frac{1}{2\tau} e^{-t/\tau} \left[1 - \cos\left(\Delta m_s \, t\right)\right] , \tag{1.1}$$

where $\tau$ is the meson's lifetime and $\Delta m_s$ is the frequency of oscillation we aim to determine.

A schematic representation of a typical $B$ event is shown in Figure 1.1. The main ingredients required by the measurement may be summarized as follows:

- *data samples:* $B$ events produced in the $p\bar{p}$ collisions need to be identified and collected, and the signal and background composition of the resulting data samples needs to be characterized,

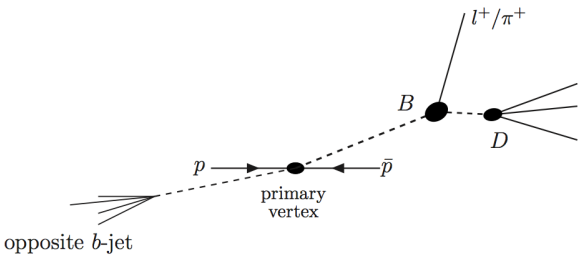


Figure 1.1: Schematic of a typical $B$ event.

- *decay time:* the proper time of the decay, $t$, is constructed from the flight distance of the meson in the detector, between the primary $p\bar{p}$ collision point and the meson's decay position, and the determination of the $B$ momentum from its decay products,
- *flavor at production and decay:* it is necessary to find what the flavor (*i.e.* $B$ or $\bar{B}$) of the meson was, both when it was produced and when it decayed, in order to determine whether it decayed as mixed (flavor of production different from flavor at the time of decay) or unmixed (flavor of production the same as flavor at the time of decay).

The above ingredients must be thoroughly characterized, with all involved quantities determined as accurately as possible and the probabilities of potential mis-determinations fully quantified.

In order to take the best advantage of the collected data samples and their characteristics a robust fitting framework is developed, which serves as the cornerstone of the data analysis. The optimal fit parameters are found using the maximum likelihood method based on the individual events input. The likelihood formulation is developed to accurately describe the characteristics of the data samples at hand, optimized for computational speed and accuracy, and implemented to efficiently accommodate the various reconstructed $B$ decay modes employed.

The data analysis is extended to the lighter $B^+$ and $B^0$ meson species, for which larger data samples are available. This allows a determination of the properties of those mesons, and simultaneously serves the purposes of method validation, tool calibration, and framework testing and development.

### Data samples

$B$ mesons originate from the hadronization of $b$ quarks produced in the proton–antiproton collisions. The $b$ production cross-section at the Tevatron is about 0.1 mb, while the total $p\bar{p}$ cross-section, including elastic, diffractive and inelastic scattering, is of the order of 75 mb.

The bottom production processes predominantly involve the creation of $b\bar{b}$ pairs. Once they have been produced, the $b$ and $\bar{b}$ quarks both undergo fragmentation forming $b$ hadrons, which include $B^+$, $B^0$, and $B_s$ mesons, as well as heavier states such as $B_c$, $\Lambda_b$, $\Xi_b$, *etc.* It should be added also that a produced $b\bar{b}$ pair in a given beam-crossing is typically accompanied by additional background interactions which are omitted in Figure 1.1.

The signature which allows one to identify $b$ hadrons from the other, more common collision products is their distinctive, long lifetimes. The $B^+$, $B^0$ and $B_s$ mesons — which constitute our aimed signal samples and which we shall commonly denote by $B$ — each have a lifetime $\tau$ of approximately 1.5 ps, or $c\tau \sim 450$ $\mu$m ($c$ denoting the speed of light). When the momentum spectrum of the $B$ mesons is folded in, the corresponding boost translates into average decay flights of the order of a few millimeters at the center of the detector, or more exactly inside the beampipe. This characteristic decay length signature is used to distinguish $B$ signals from the myriad of background processes with their much larger cross-sections. Such characteristic secondary vertices are explored, as a matter of fact, already at the level of real-time event selection, or *trigger*ing. The daughter particles which originate from $B$ decays usually have significant impact parameter with respect to the primary interation vertex, as illustrated in Figure 1.2. The reconstructed trajectory of a long-lived (*e.g.* pion, kaon) charged particle, dubbed *track*, is said to be "detached" if the impact parameter, divided by its uncertainty, is large. CDF possesses a trigger processor which performs fast and precise track reconstruction based on information from the Silicon detectors, which is capable of looking for the presence of such detached tracks. This capability is central to the trigger strategy employed for gathering the majority of the samples used in the analyses. The detachment requisite is complemented by further topological and kinematical event information. More traditional trigger criteria based on the presence of leptons with moderate to high transverse momenta are also concurrently explored.

The $B$ mesons are reconstructed in a variety of final states. These may be classified as corresponding to fully- or partially-reconstructed $B$ decays. In the former case, one attempts to identify all particles participating in the decay, as for instance in $B \to D\pi$. The latter class includes for example decays of the type $B \to Dl\nu$, where one does not attempt to reconstruct the neutrino which escapes detection. The designations of *hadronic* and *semileptonic* decays will correspondingly be also employed to refer to the two classes. The leading Feynman diagrams associated with the mentioned example decays are shown in Figure 2.1. In general the semileptonic modes will have considerably larger (∼10-fold) yields, while the samples' composition will be also more complex and difficult to assess. The hadronic samples despite having smaller yields provide a more complete information about the $B$ meson, most notably its momentum.

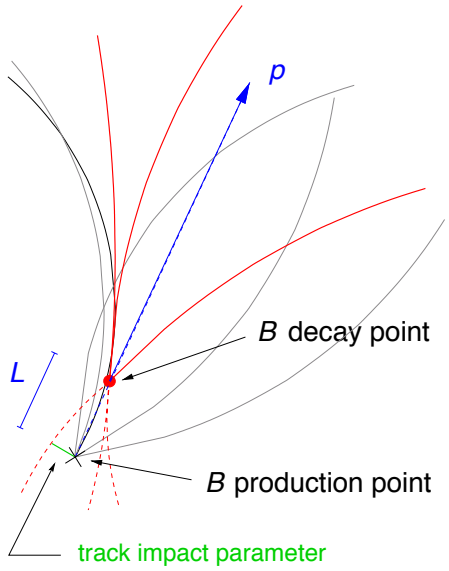


Figure 1.2: Sketch of a $B$ decay.

The gathered samples of reconstructed $B$ candidates will contain, in addition to the aimed signals, background events from various sources. The most harmful backgrounds are those which peak in the signal region (of a discriminating variable, for instance the candidate's mass) and which can more easily fake signals. The background sources and their characterization are specific to the individual decay modes. In the case of the semileptonic samples, not only is the signal and background separation complicated by the fact that the $B$ momentum, and thus its mass, is not fully accessible, but furthermore a same lepton-$D$ final state may in fact be achieved as the product of various $B$ mesons' decay chains which are not differentiated. The signal composition and, more generally, the characterization of physics-like background contributions from processes other than the nominally reconstructed decay mode benefit from Monte Carlo simulation of the relevant processes.

An overview of the CDF detector and its trigger system is provided in Chapter 3. The reconstruction of the $B$ mesons' candidates and the characterization of the corresponding samples are explained in Chapter 4. The full collection of decay modes studied is summarized in Table 4.1.

### Proper decay time

The proper decay time of a $B$ meson candidate is calculated from the decay distance $L$ between the production and decay points, the momentum $p$, and the meson's nominal mass $M^B$, as $t = L/\gamma\beta c = LM^B/p$. In fact, the projections of both the distance and the momen-

tum on the plane transverse to the beamline are used. The proper time probability density function (PDF) is determined by the $B$ meson lifetime (2.1),

$$\mathcal{P}(t) \sim \frac{1}{\tau} e^{-t/\tau} \ . \tag{1.2}$$

The above expression becomes modified once various necessary correcting and resolution effects are accounted for. These include the limited precision with which the $B$ decay length can be measured. The incomplete momentum reconstruction in the case of the semileptonic modes induces further smearing of the PDF; this smearing effectively translates into an additional contribution to the proper time uncertainty (11.4). The detachment requirements employed for event selection and reconstruction also introduce a modification in the shape of the $t$-PDF which needs to be appropriately described.

The proper decay time likelihood description for the various samples and the calibration of the corresponding uncertainty are contained in Chapter 5. The lifetimes of the $B$ mesons are measured; this also constitutes a final validation of the description of the samples before the introduction of flavor tagging information.

**Flavor tagging**

Determining the flavor of a $B$ meson is equivalent to determining its $b$ or $\bar{b}$ quark content. In general, flavor tagging exploits a correlation between the beauty flavor of the $b$-hadron and a *charge* in the event. The $B$ mesons are reconstructed in flavor-specific final states. It follows that the flavor at the time of decay is given by the electric charges of the decay products. For example, a $B_s$ decays to $D_s^- \pi^+$ or $D_s^- l^+ X$, while a $\bar{B}_s$ decays into $D_s^+ \pi^-$ or $D_s^+ l^- X$.

The flavor at the time of production is more difficult to ascertain, rendering its determination a more complex task. Several different flavor tagging techniques are used for that purpose, being associated to two general strategies. The *opposite side* tagging (OST) methods exploit the fact mentioned above that bottom quarks are predominantly produced in $b\bar{b}$ pairs. These techniques thus aim at inferring the $B$ meson production flavor by identifying the flavor of the second, accompanying $b$ quark. Specifically, these techniques correspond to the *soft lepton* taggers, which attempt to identify electrons or muons from semileptonic $b$-decays, and the *jet charge* taggers which explore properties of clusters of tracks to statistically infer (the sign of) the $b$ charge.

The *same side* tagging (SST) technique is based on correlations between particles produced in the fragmentation of $b$ quarks to the $B$ mesons. The SST algorithms, unlike the OST counterparts, are based on information carried by tracks found in the vicinity to the $B$ meson being tagged. The SST performance, also unlike the OST case, is expected to vary

among $B$ species. In the case of $B^+$ and $B^0$, the mentioned charge-flavor correlations are enhanced by decays of $P$-wave $B$ mesons ($B^{**}$). For the $B_s$ mesons, the leading fragmentation track expected to be correlated to the $B$ flavor is a kaon, and the algorithm's performance is thus enhanced by making use of information allowing the separation of kaons from the more abundant pions.

A given flavor tagging algorithm does not always provide a correct decision about the $B$ meson flavor. A method's performance is conveniently quantified in terms of its tagging efficiency $\epsilon$ and dilution $\mathcal{D}$. The efficiency is the fraction of signal candidates with a flavor tag. The dilution is defined as $\mathcal{D} \equiv 1 - 2w$, where $w$ is the mistag probability; in this way, a perfect tag would have unit dilution, while a random tag would have zero dilution. Besides the tag decision also the probability of its correctness, or equivalently the dilution, must be evaluated for the individual events. The figure of merit of a tagging algorithm is given by $\epsilon\mathcal{D}^2$.

The tagging methods are presented in detail in Chapter 6, while in Chapter 9 a novel SST method is further developed for suitably tagging the flavor of $B_s$ mesons.

### Mixing

The proper decay time PDF describing flavor oscillations may be expressed as

$$\mathcal{P}(t) \sim \frac{1}{2\tau} e^{-t/\tau} \left[1 \pm \mathcal{A}\mathcal{D} \cos\left(\Delta m\, t\right)\right] . \tag{1.3}$$

This is simply a slight elaboration of (1.1). The signs "+" and "−" refer to $B$ candidates identified as unmixed and mixed, respectively. This identification is achieved with the flavor tagging methods, whose dilution $\mathcal{D}$ is provided to the fit, for each event, and is found to attenuate the oscillating term given by the cosine. The parameter $\mathcal{A}$ is introduced as describing the amplitude of the oscillation and is, for the moment, taken as unity.

Two mathematically equivalent methods are employed to extract information about the oscillation frequency $\Delta m$ from the data. The first method involves performing a fit to the parameter $\Delta m$ directly. In this way, the oscillation frequency is treated as a standard fit parameter, whose best estimate is found by maximizing the likelihood function for the data sample at hand, and whose uncertainty is determined by the variation of the likelihood function around the found maximum. This constitutes our chosen method for the measurement of the oscillation frequency in the $B^0$ system performed in Chapter 7. In fact, the fit is performed simultaneously for $\Delta m$ and for the parameter $\mathcal{A}$, where the later constitutes in this case a calibrating factor of the dilution of the flavor tagging methods when applied to the actual mixing samples.

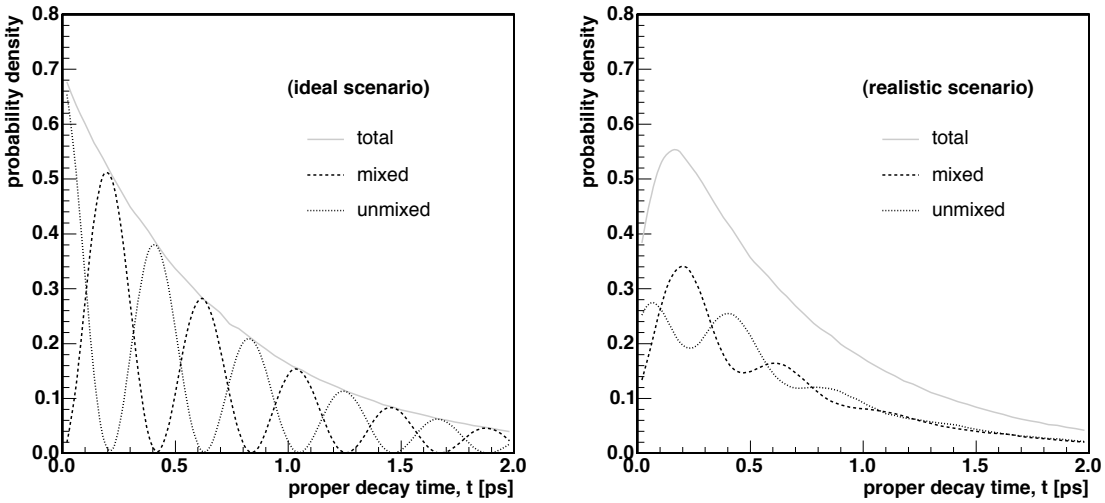


Figure 1.3: Realistic effects on the oscillation signal: *i*) ideal scenario, for an oscillation frequency of $15\,\mathrm{ps}^{-1}$ (left), and *ii*) the resulting signal after selection bias, decay length and momentum resolutions (right).

The second method for extracting information about the oscillation frequency is to determine the amplitude $\mathcal{A}$ as a function of the frequency which itself is fixed, at each step, to a different probe value. The method is appropriate for searching for fast oscillations, making it convenient for evaluating exclusion conditions on individual frequency values. A frequency point is excluded to a given confidence level (C.L.) if the hypothesis $\mathcal{A} = 1$ is excluded in a one-sided Gaussian test. Specifically, all values of $\Delta m$ for which the combined variable $\mathcal{A} + 1.645\sigma_{\mathcal{A}}$ is smaller than 1 are excluded at 95% C.L., where $\sigma_{\mathcal{A}}$ is the total uncertainty on $\mathcal{A}$. The exclusion limit is defined as the largest frequency value below which all frequencies are excluded. The sensitivity for 95% C.L. is given by the range where $1.645\ \sigma_{\mathcal{A}} < 1$, *i.e.* it corresponds to the expected limit if an average observed amplitude $\mathcal{A} = 0$ (expected in the absence of oscillation) would be obtained. This is the method used in Chapter 8 for scanning for $B_s$ oscillations. It allows as well a more straightforward combination of results from different analyses.

The necessary modifications stemming from resolution and bias effects mentioned above regarding the lifetime PDF (1.2) hold equally for the mixing PDF (1.3). The latter is represented in Figure 1.3 before and after resolution, bias and mistagging effects. These effectively cause the dampening of the oscillations.

The statistical significance of an oscillating signal may be approximated (11.17) by

$$\left(\begin{smallmatrix}\text{mixing}\\ \text{significance}\end{smallmatrix}\right)^2 \sim \frac{\epsilon \mathcal{D}^2\, S}{2} \cdot \frac{S}{S+B} \cdot e^{-\sigma_t^2 w^2}\ , \tag{1.4}$$

| | $K^0\bar{K}^0$ | $B^0\bar{B}^0$ | $B_s\bar{B}_s$ |
|---|---|---|---|
| mass [MeV/c$^2$] | $497.648 \pm 0.022$ | $5279.4 \pm 0.5$ | $5369.6 \pm 2.4$ |
| lifetime [ps] | $89.53 \pm 0.06$, $51800 \pm 400$ | $1.536 \pm 0.014$ | $1.461 \pm 0.057$ |
| $\Delta m$ [$(\hbar/c^2)s^{-1}$] | $(0.5292 \pm 0.0010) \cdot 10^{10}$ | $(0.507 \pm 0.005) \cdot 10^{12}$ | $> 14.4 \cdot 10^{12}$ |
| $\Delta m$ [eV/c$^2$] | $(3.483 \pm 0.006) \cdot 10^{-6}$ | $(3.337 \pm 0.033) \cdot 10^{-4}$ | $> 94.8 \cdot 10^{-4}$ |

Table 1.1: Parameters of the oscillating kaon and bottom meson systems.

where $S$ and $B$ are the number of signal and background events in the selected sample and $\sigma_t$ stands for the resolution on the proper decay time. The effective signal yield of the sample is seen to be scaled down by the tagging power $\epsilon\mathcal{D}^2$ which quantifies the limited performance of the flavor tagging algorithms employed. The effect of the proper decay time resolution is observed to be determining as well, particularly so in the case of higher oscillation frequencies. This allows one to anticipate the complementarity of the hadronic and semileptonic samples. The relatively large yields of the latter are expected to provide the dominant contributions to the lower range of the probed frequency spectrum, while the precise resolutions which characterize the former samples are expected to contribute the most discerning power at higher frequencies. The expression (1.4) can be used to estimate the sensitivity of the sample given its relevant characteristics. In Section 11.2 this is used to quantify expected sensitivity increases in view of improvements such as in flavor tagging and the increasing samples' size.

**Constraining the CKM parameters**

The obtained oscillation frequency information may be combined with other pieces of experimental and theoretical information relevant to infer the parameters of the unitarity triangle within the CKM framework. This is explored in Chapter 12. The various constraints are combined to form an inference framework based on Bayesian probability. The basic idea is that beliefs (*i.e.* probabilities) on the value of each input quantity are propagated into beliefs about the output quantities, such as the $\bar{\rho}$ and $\bar{\eta}$ CKM parameters. Such *posterior* probabilities can also be obtained for the input quantities themselves. The inference procedure may be carried out both including and excluding selected inputs, such as $\Delta m_s$, thus emphasizing its constraining effect.

## 1.2 History note

Particle–antiparticle oscillations have been established in other neutral meson systems. The oscillation frequencies are very well measured for the $K^0$ and $B^0$ systems, while for the $B_s$ the oscillations are very rapid and their frequency had yet to be detected.

Oscillations were first proposed for the kaon system in 1955 [16]. This lead to predicting the existence of a long-lived strange particle, the $K^0_L$, which was subsequently observed in 1956 [17]. The first CKM element, the Cabibbo quark mixing angle identified with $\theta_{12}$ in (2.39), was introduced in 1963 [4] to explain the small decay rates for particles carrying strangeness. This further lead in 1970 to the introduction of the unitarity quark mixing ansatz used by GIM [18] to postulate the existence of a fourth quark (charm). In 1973 Kobayashi and Maskawa [5] added to the model a third generation of quarks, motivated by the earlier discovery of CP violation in 1964 in $K^0$ decays [19]. The bottom and top quarks were subsequently discovered in 1977 [20] and 1995 [21], respectively, at Fermilab.

Evidence of neutral $B$ meson mixing was first reported in 1987 by UA1 [22]. This consisted of a time-integrated analysis, based on the measurement of the ratio of like-sign muon pairs to unlike-sign muon pairs. The first observation of $B^0$ oscillations was published by ARGUS [23] in that same year, and included the unambiguous identification of a $B^0B^0$ pair. Confirmation of those results was provided by CLEO [24] in 1989. Various other time-integrated mixing analyses followed, at PEP, PETRA, and LEP experiments, as well as at CDF. Time-dependent measurements of $B^0$ mixing have since then yielded a precise determination of the oscillation frequency $\Delta m_d$. A compilation is presented in Figure 1.5. The world average value for $\Delta m_d$ is $0.507 \pm 0.005$ ps$^{-1}$ [25], being dominated by BaBar and Belle measurements [26].

That $B_s$ mesons undergo oscillations could be inferred from early measurements. The above mentioned measurements by ARGUS and CLEO, which operate at $e^+e^-$ colliders tuned to the $\Upsilon(4S)$ resonance, provided the time integrated probability that a $B^0$ oscillates. When these were compared with inclusive measurements performed at LEP, for instance, where in addition to $B^0$ also $B_s$ mesons are produced, a significant contribution to the mixing signal from the latter was deduced. Subsequent time-dependent measurements, performed at LEP and SLD operating at the $Z$-pole, and at CDF in the previous data taking stage of the Tevatron operating at an energy $\sqrt{s} = 1.8$ TeV, established lower exclusion bounds on the oscillation frequency of the $B_s$ system.

For the purpose of combining exclusion regions from the various experiments in a convenient and consistent fashion, the results on $B_s$ oscillations are presented in terms of amplitude measurements for a spectrum of probe frequencies. Such a procedure [33] essentially entails

searching for a peak in the power spectrum of the data as a function of frequency. The combined results prior to the CDF II contribution are presented in Figure 1.6, giving a world average exclusion limit of $\Delta m_s > 14.4$ ps$^{-1}$ at 95% C.L. [25]. Contributions from ALEPH, DELPHI, OPAL, SLD, and CDF I are included. The corresponding combined sensitivity given by the measured amplitude uncertainties is 18.2 ps$^{-1}$.

In Table 1.1 we summarize the values of $\Delta m$ for the kaon and bottom neutral systems. While it may well be expressed in units of mass, $\Delta m$ will be revealed in the data as an oscillaiton frequency. Accordingly, througout this document, unless otherwise specified, the $\Delta m$ observable will be expressed in units of inverse-(pico)second.

Expectations for $\Delta m_s$ may be derived within appropriate theory-based frameworks. In particular, global fits to the standard model relations, connecting the CKM elements with the various experimental observables and theory calculations, have been performed, and resulting expectations produced. A summary of such predictions spanning more than a decade is illustrated in Figure 1.4 [82].

The first preliminary results from the Tevatron experiments appear by the summer conferences 2005 [31]. These yield already significant contributions to the combined world averages. In March of 2006, the DØ Collaboration reported direct limits on the $B_s$ oscillation frequency [92]. Using a sample of $B_s \to D_s l$ partially reconstructed decays, in a dataset of 1fb$^{-1}$ integrated luminosity, the lower limit $\Delta m_s > 14.8\,\mathrm{ps}^{-1}$, at 95% C.L., was obtained along with an analysis sensitivity of $14.1\,\mathrm{ps}^{-1}$. A direct two-sided bound, $17 < \Delta m_s < 21\,\mathrm{ps}^{-1}$ (90% C.L.), was also reported. The measured amplitude scan is shown in Figure 1.7.

In June of 2006, based on a $1\,\mathrm{fb}^{-1}$ data sample of partially and fully reconstructed decays, the CDF Collaboration reports [101] the first measurement of the $B_s$ oscillation frequency $\Delta m_s = 17.31^{+0.33}_{-0.18}(\mathrm{stat.}) \pm 0.07(\mathrm{syst.})\,\mathrm{ps}^{-1}$. Three months later, in September 2006, an updated iteration of the same analysis, applied to the same $1\,\mathrm{fb}^{-1}$ dataset and after incorporating few additional refinements, yielded a further precise measurement [101], $\Delta m_s = 17.77 \pm 0.10(\mathrm{stat.}) \pm 0.07(\mathrm{syst.})\,\mathrm{ps}^{-1}$. The probability that random fluctuations could produce a comparable signal was estimated to be $8 \cdot 10^{-8}$, corresponding to a significance in excess of $5\,\sigma$. The CDF analysis corresponds accordingly to the first, long-sought, definitive observation of $B_s$ oscillations.

In Figure 1.8 the amplitude measurements, at the specified probe frequency, performed by various experiments are compared. In Figure 1.9 the CDF amplitude scan is compared to the world combined results. The overshadowing contribution of the CDF analysis is striking. The stated purpose of the current monograph is to provide the detailed description of the analysis developed and carried out at CDF.

At the moment the current research took place, the Tevatron was the only particle col-

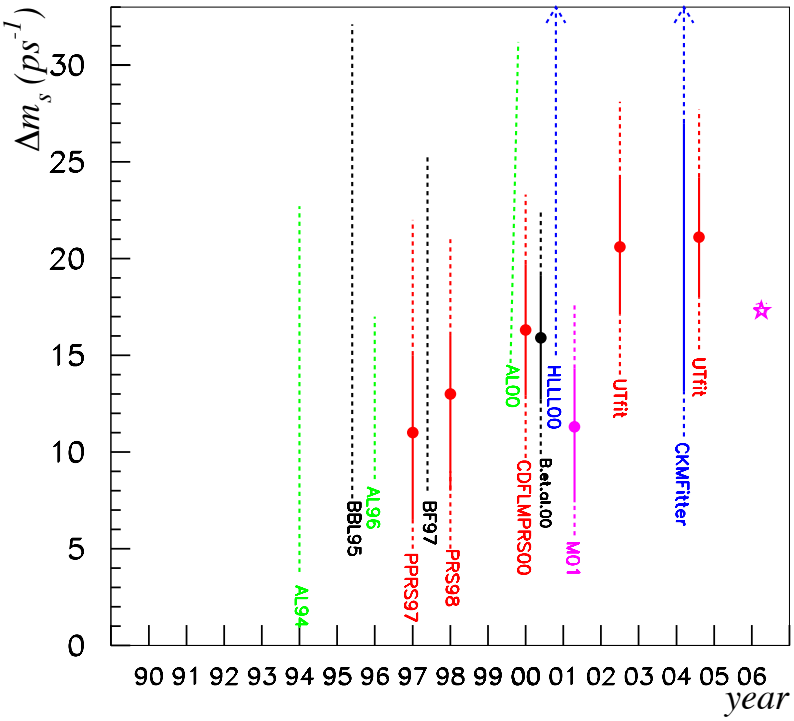


Figure 1.4: History of $\Delta m_s$ predictions.

lider producing significant samples of $B_s$ mesons. The CDF and DØ collaborations stood therefore in unique positions to explore the $B_s$ system. A first and precise determination of its oscillation frequency, or the exclusion of the SM favored region, was a stated priority of the Tevatron Run II physics program.

The $B_s$ meson is too heavy to be produced in decays of the $\Upsilon(4S)$ resonance, and cannot thus be studied at the $B$ factories which operate at that energy. The kinematical threshold is satisfied though by the $\Upsilon(5S)$ resonance, which may be explored. For instance, the asymmetric $e^+e^-$ KEKB collider was recently operated at this resonance in an engineering run, which allowed the Belle experiment to take first $B_s$ data [32]. The excitement of further studying the $B_s$ meson is expected to be transferred in the future to the Large Hadron Collider (LHC) experiments at CERN – namely LHCb, and also ATLAS and CMS. Not only will it be possible to corroborate the Tevatron results to a higher precision, but novel flavor measurements will be achievable. The exploration of the $B_s$ system undertaken at the Tevatron will accordingly be complemented and deepened at the LHC.

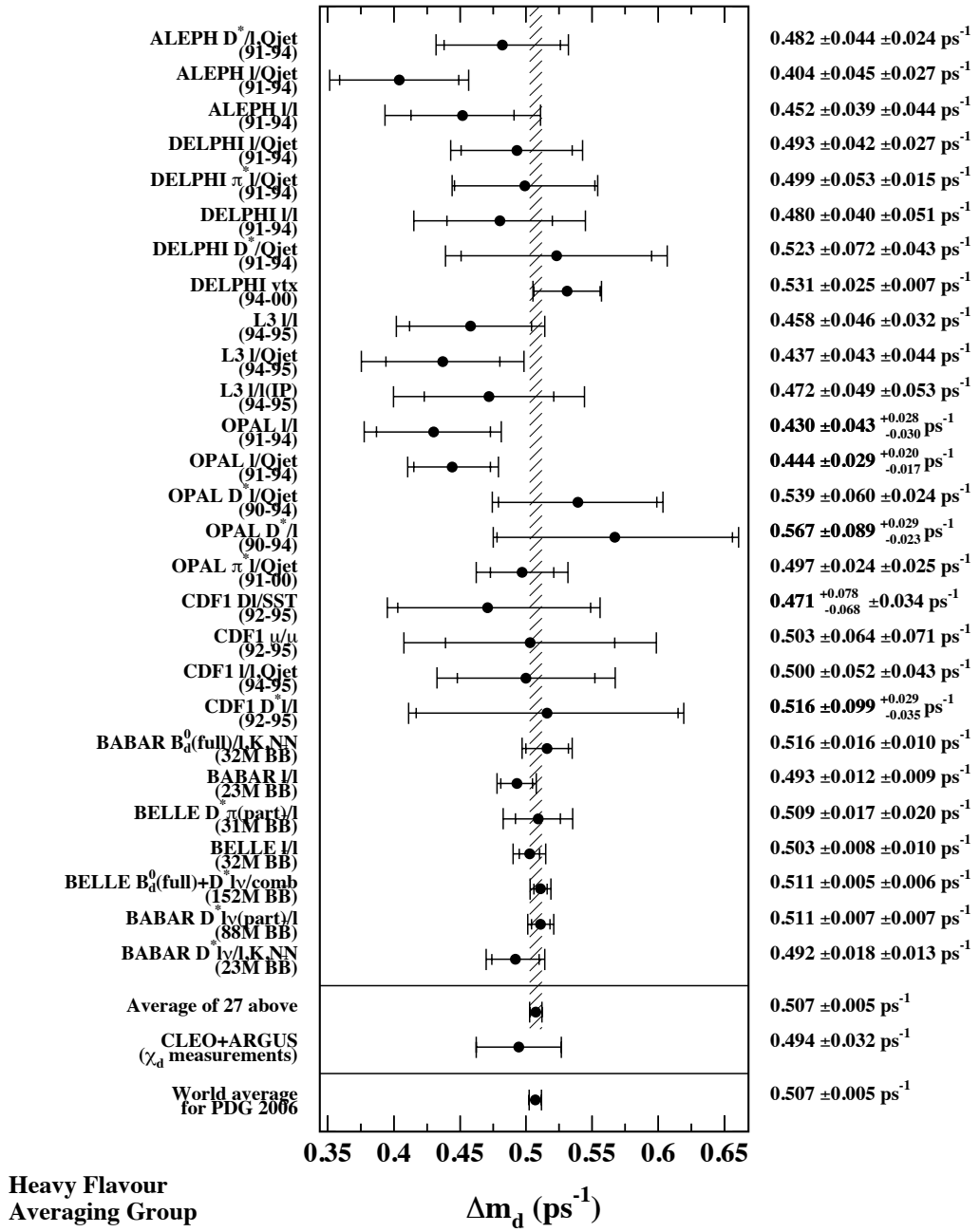


Figure 1.5: Experimental measurements of $\Delta m_d$.

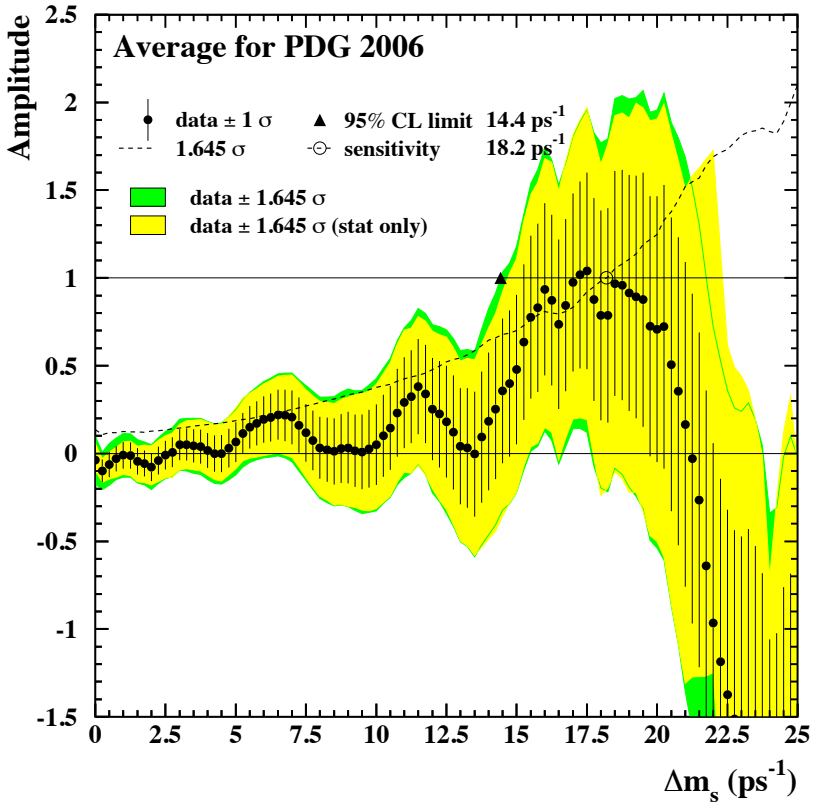


Figure 1.6: World combined amplitude results on $B_s$ oscillations, prior to the CDF II measurement.

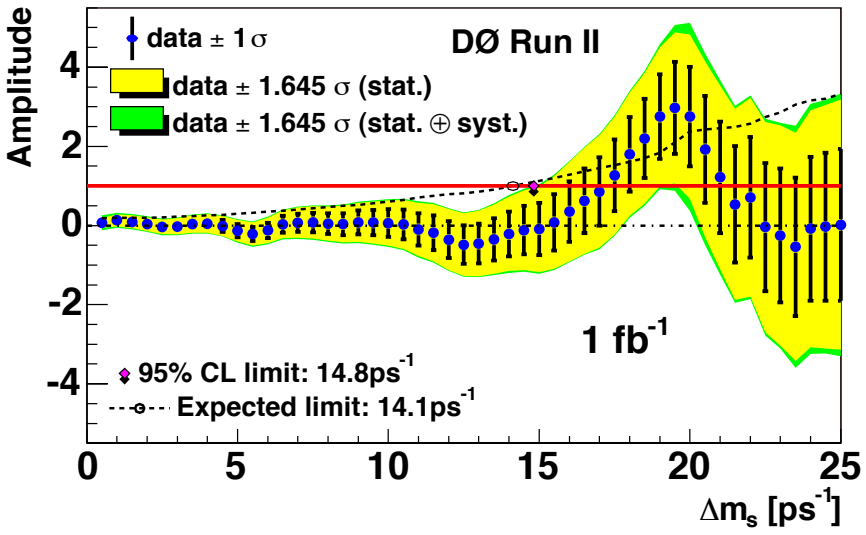


Figure 1.7: Amplitude scan reported by the DØ Collaboration.

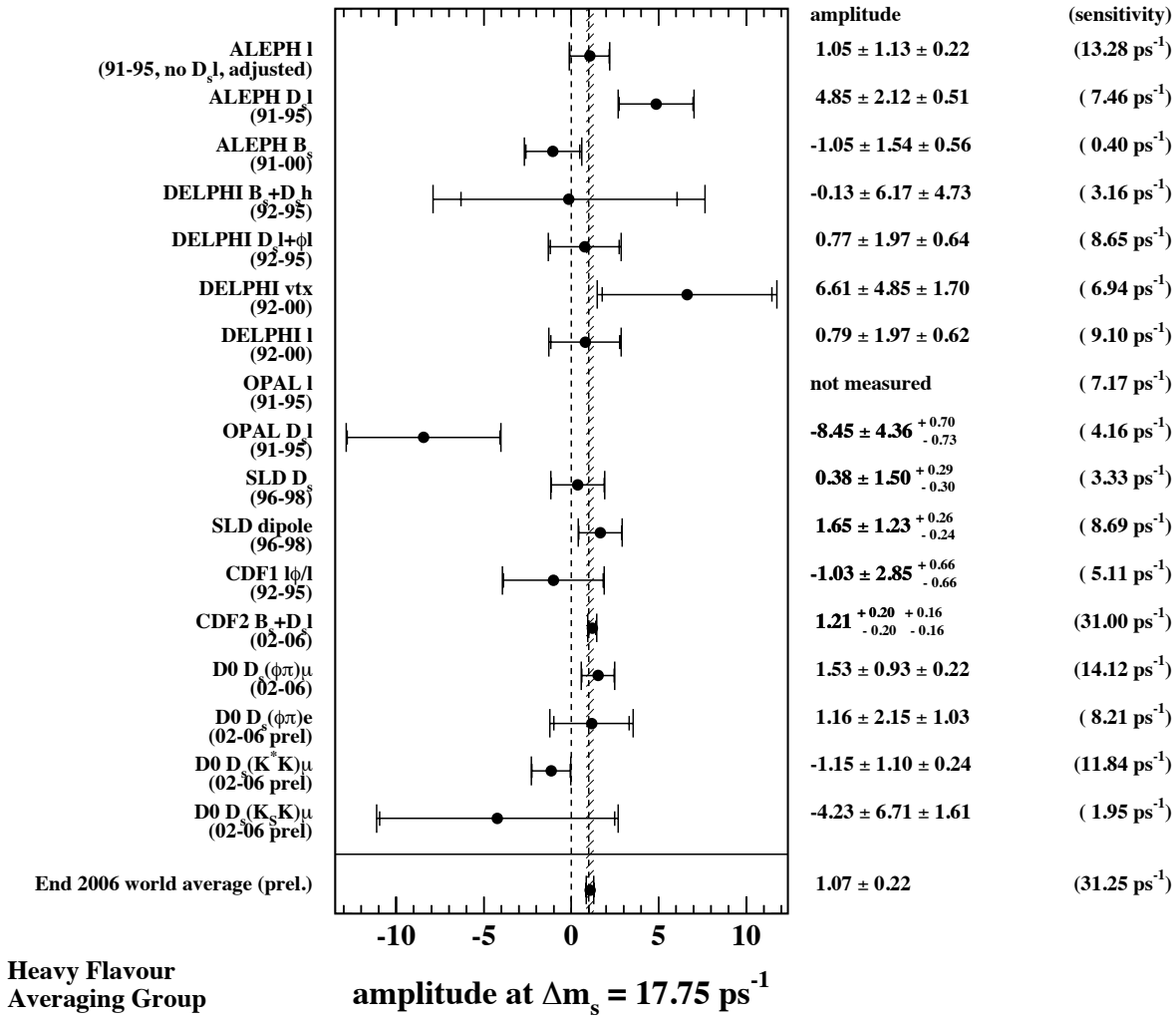


Figure 1.8: Experimental amplitudes and sensitivities at the $\Delta m_s$ probe frequency 17.75 ps$^{-1}$.

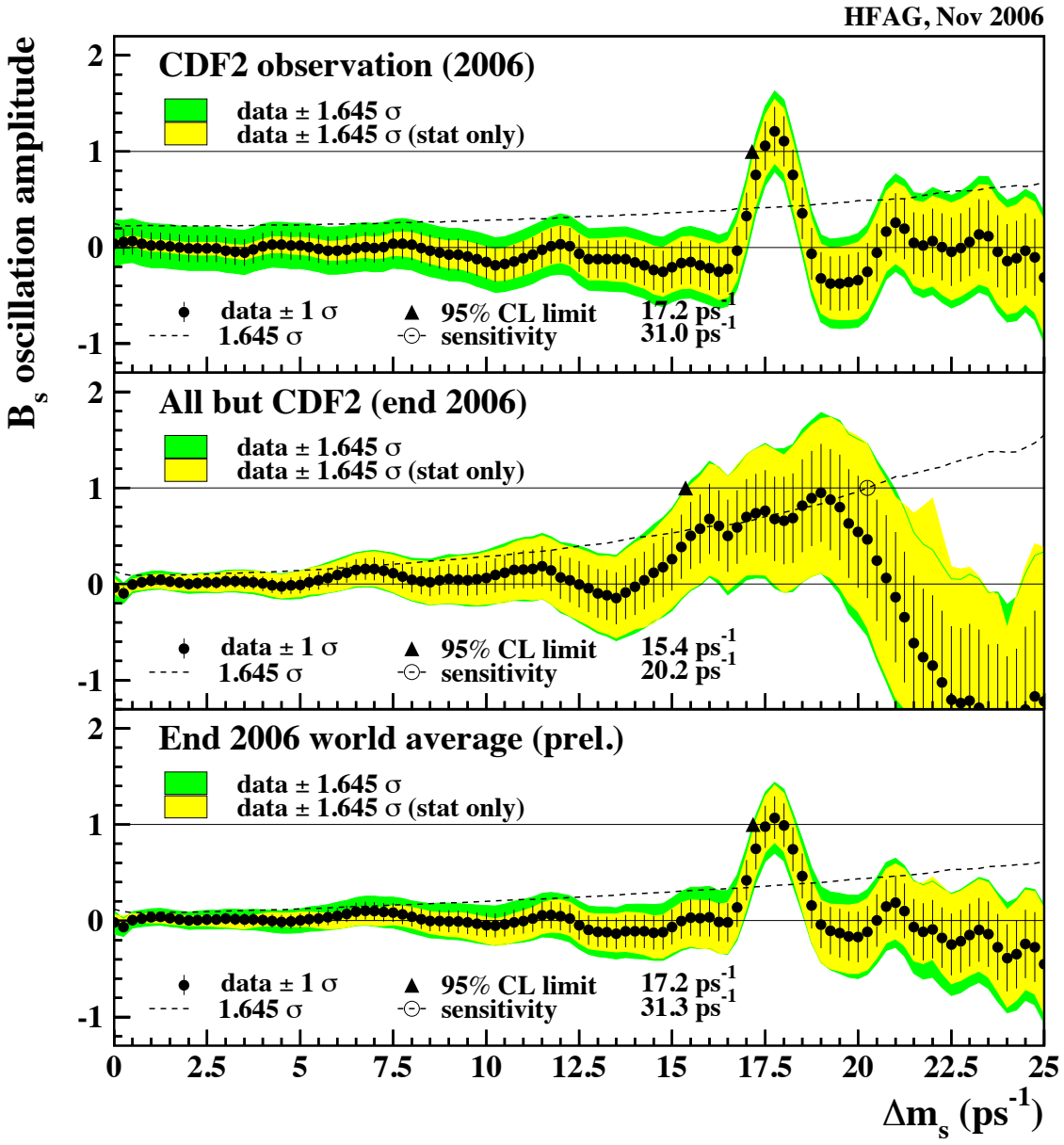


Figure 1.9: Amplitude scan showing the CDF measurement and comparison to the world combined results.